MAGNETO
Control Interface for Autonomous Delivery of Magnetically Stimulated Particles

Victor Huynh, Bassam Mutawak, Minh Quan Do, Elizabeth Ankrah | Dr. Nathalia Peixoto, Dr. Qi Wei, Dr. Lamar Mair
Department of Bioengineering, George Mason University Volgenau School of Engineering | Weinberg Medical Physics, LLC.

Abstract

Background:
Magnetic Particle Delivery is the *in vivo* transport of nanocarriers via external magnets. Although it is a promising method for the noninvasive delivery of therapeutic payloads, many limitations (e.g. physiological barriers, magnetic field attenuation, impracticality of manual control) are holding the technology back from clinical implementation [1]. Weinberg Medical Physics (WMP) is constructing an MRI-guided magnetic control system (MCS) to overcome these limitations [2].

Purpose:
(1) Design and build a precursor software control interface for WMP's future MCS. The software will control WMP's 4 coil array MCS as a test platform.

(2) Improve control of the 4 coil array MCS by automating and increasing accuracy of its particle translation.

Significance:
MAGNETO lays the foundation for automation behavior, control flow, and user interaction for future MCS.

Technical Requirements

Graphical User Interface (GUI)

- Optical image streaming at > 30 fps
- Consistent object-of-interest detection against various lighting
- 2D user path drawing and processing (e.g. discretization, loading/saving)
- Particle delivery automation protocol (e.g. sequence of events, safety features)
- Real-time data collection (particle translation fields, UI high-level interactions)

Particle Control

- Bidirectional hardware communication with GUI
- Operating system independent control scheme
- Simultaneous control of multiple hardware components
- Consistent translation across user-defined path

System Operation

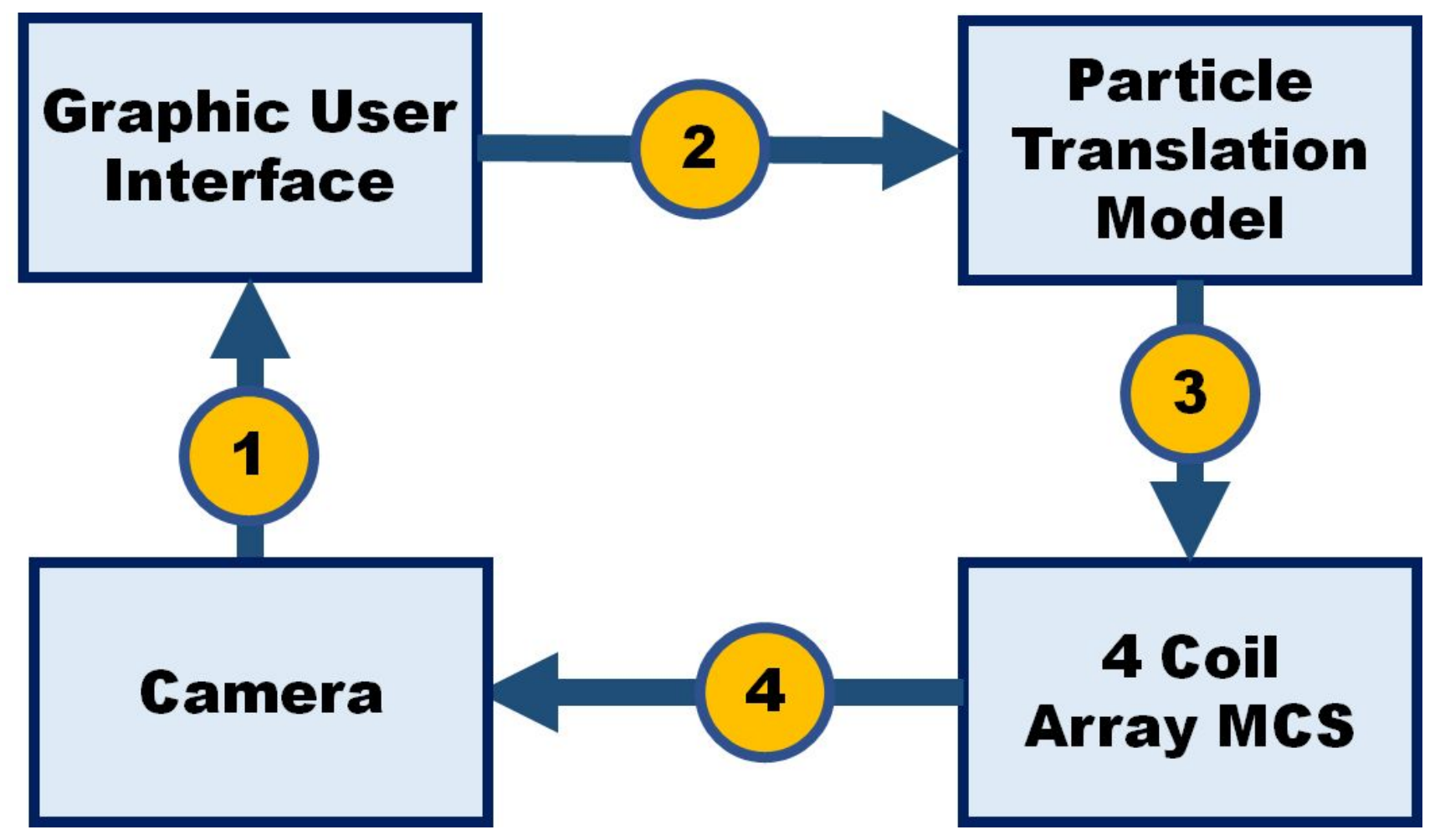

Figure 1. High-level diagram of system operation. After the user performs basic setup, the system will run this cycle autonomously until delivery completion or user discretion.

1. **Camera** streams images of the hardware setup to the GUI software.
2. **Graphical User Interface (GUI)** performs image segmentation on received images to detect the magnetic particle and update the delivery progress. Particle location and path information is then fed into the Particle Translation Model.
3. **Particle Translation Model** uses location parameters to calculate the necessary electrical current (in each coil) needed for the system to perform the desired translation. Feedback features using information from previous translations are serve to both augment and regulate the model's outputs.
4. **4 Coil Array MCS** uses motor controllers to apply current to the connected solenoid coils. Different currents can be applied simultaneously to multiple coils. All particle translation is detected by the camera.

Graphic User Interface

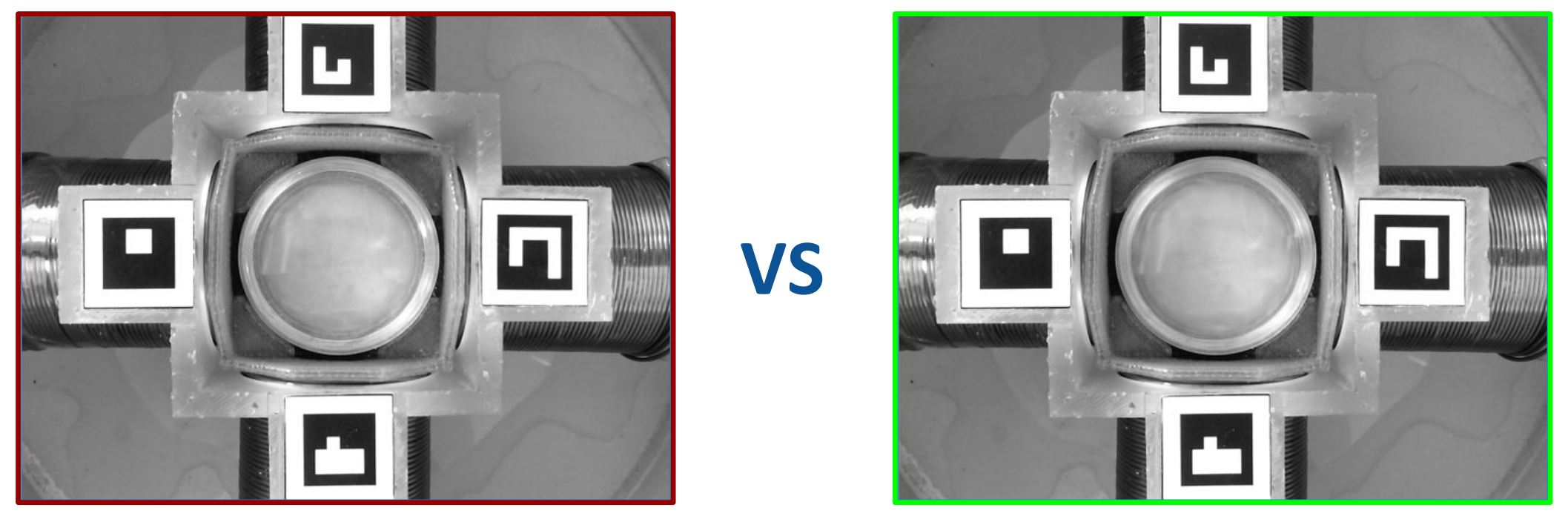

Figure 2. Selected strategy for image segmentation is modified image subtraction. Typical implementation requires a background image without presence of the object-of-interest (left). Our implementation synthesizes the image by performing averaging over a calibration period in which the ball in constantly kept in motion (right).

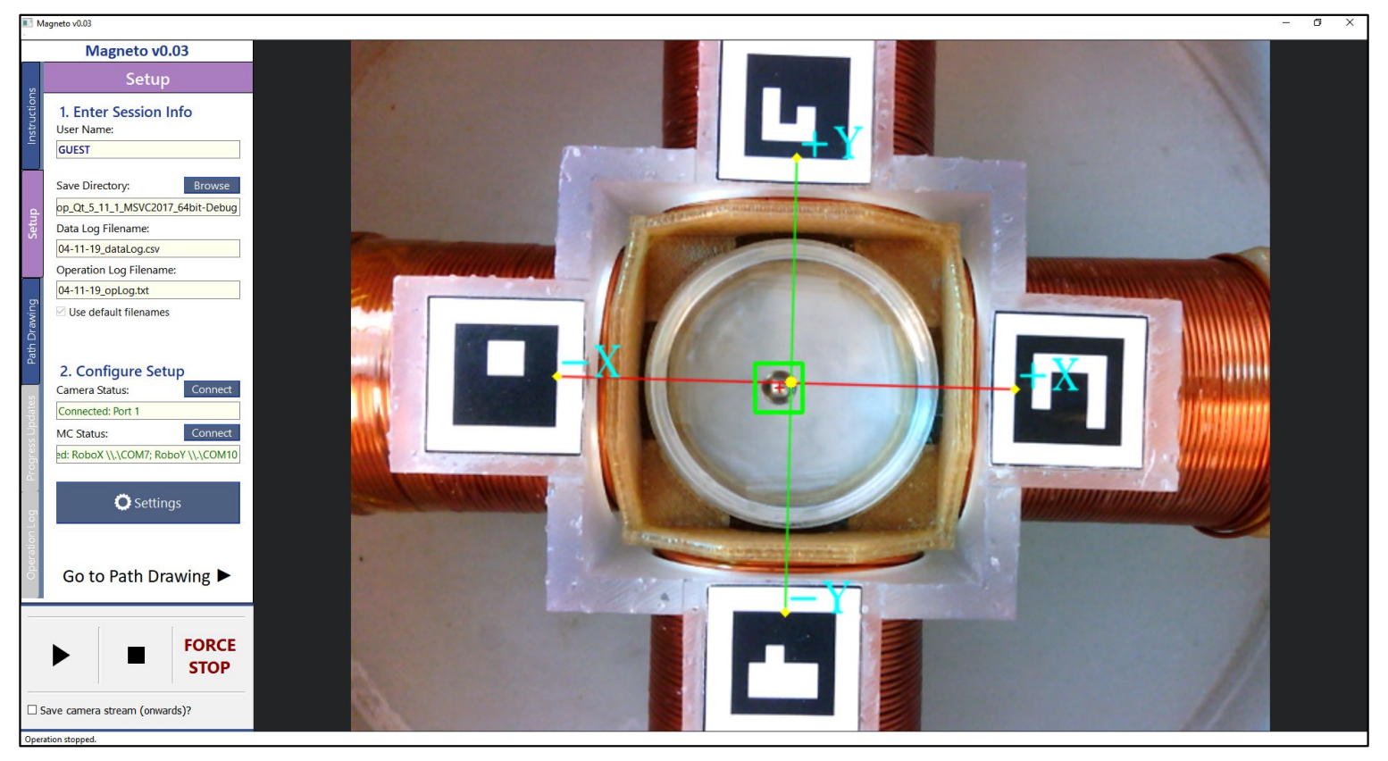

Figure 3. GUI setup is streamlined into simple, fast steps. These include specifying a data save directory, connecting hardware, and confirming particle detection via user-set parameters..

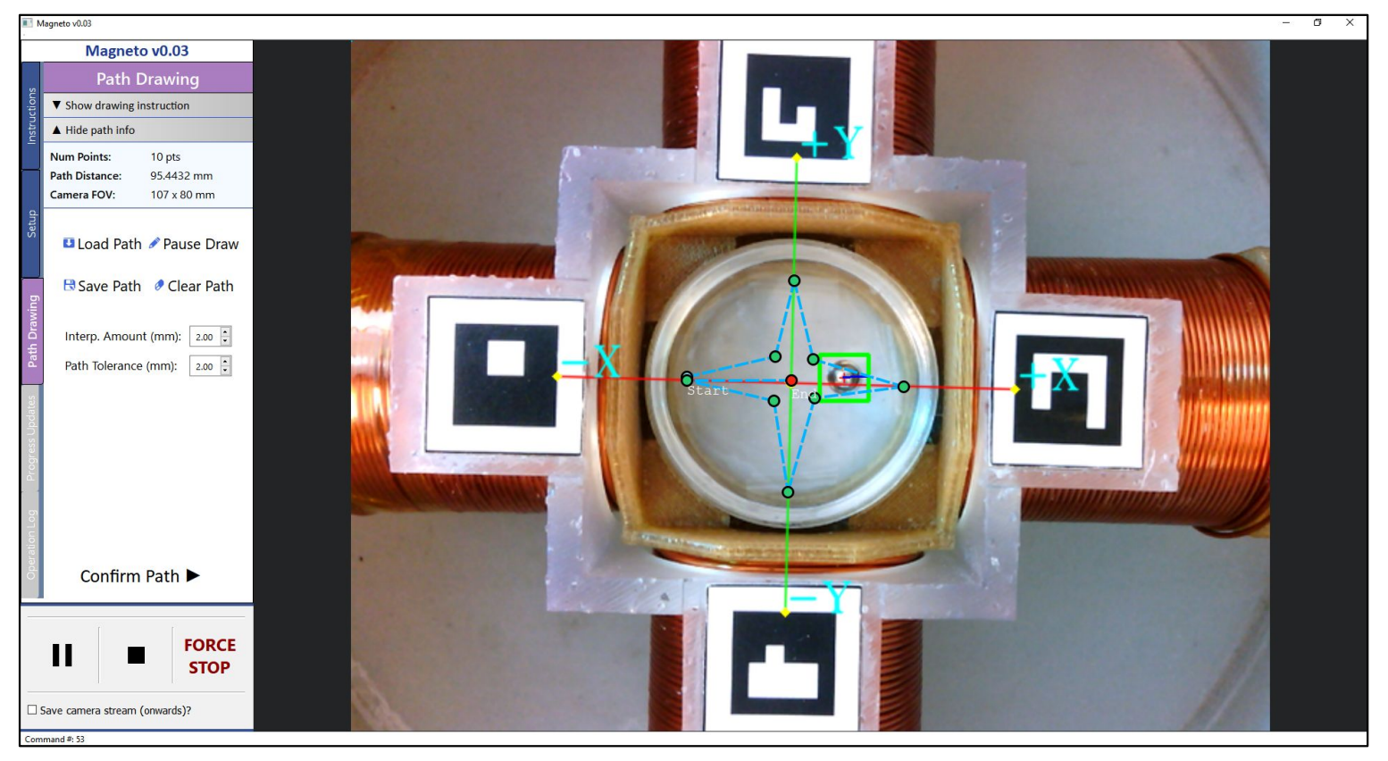

Figure 4. Path drawing allows for dragging-dropping of points and loading and saving paths. Users can set the level of interpolation and translation deviation.

Translation Model

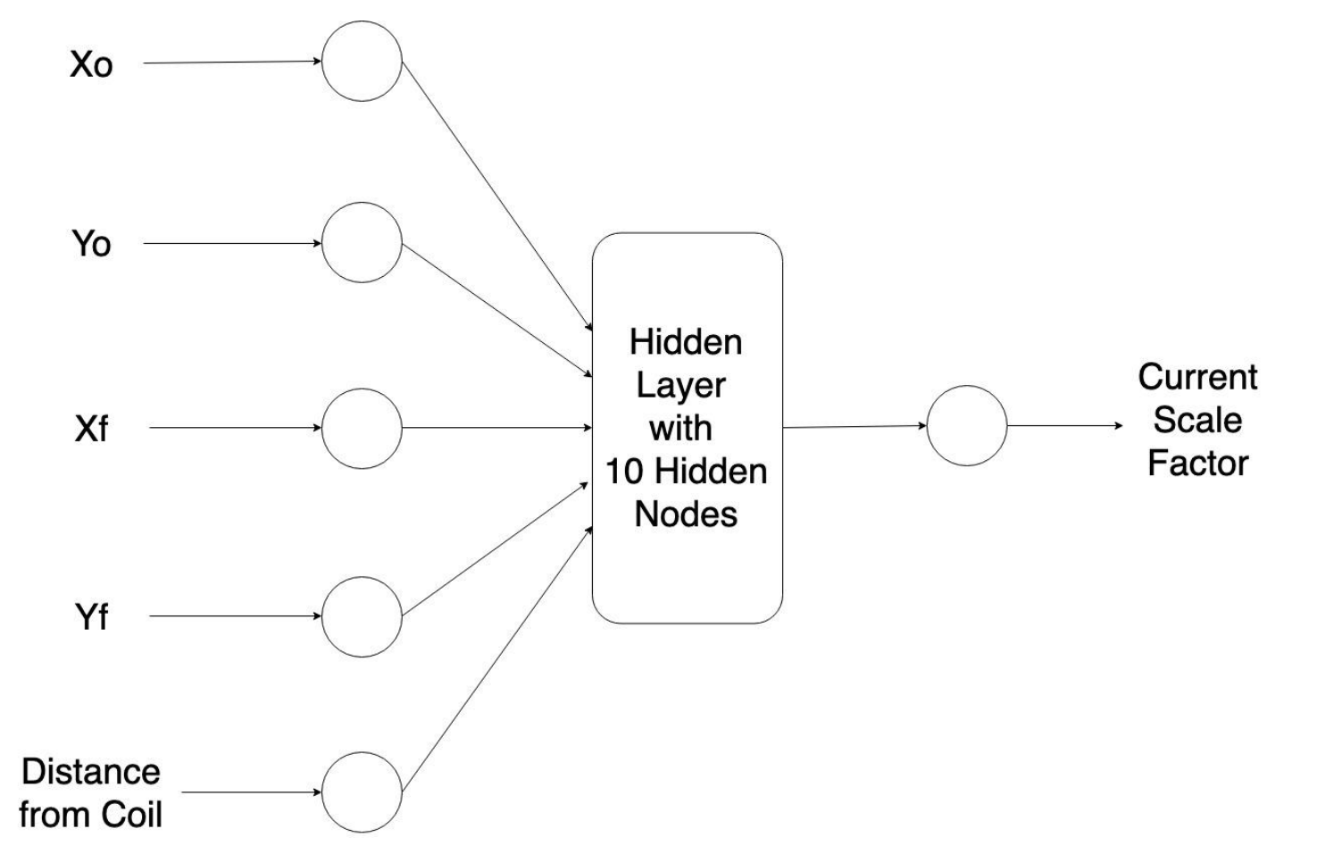

Figure 5. Neural network architecture for a single coil. Inputs are initial and final coordinates as well as the distance from coil. Output is current scale.

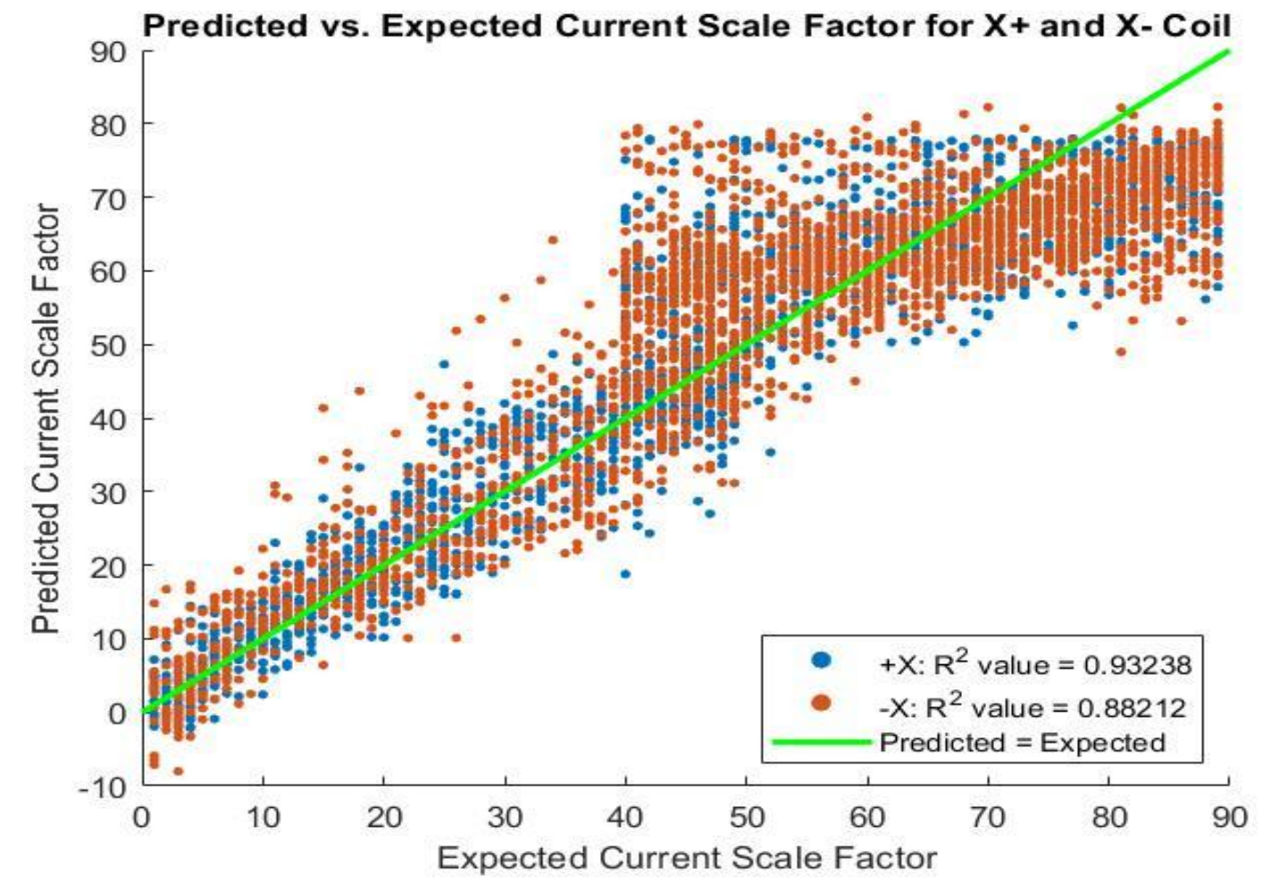

Figure 6. Training regression plot. An ideal regression fit would predict the expected current scale factor with 100% accuracy ($R^2 = 1.0$).

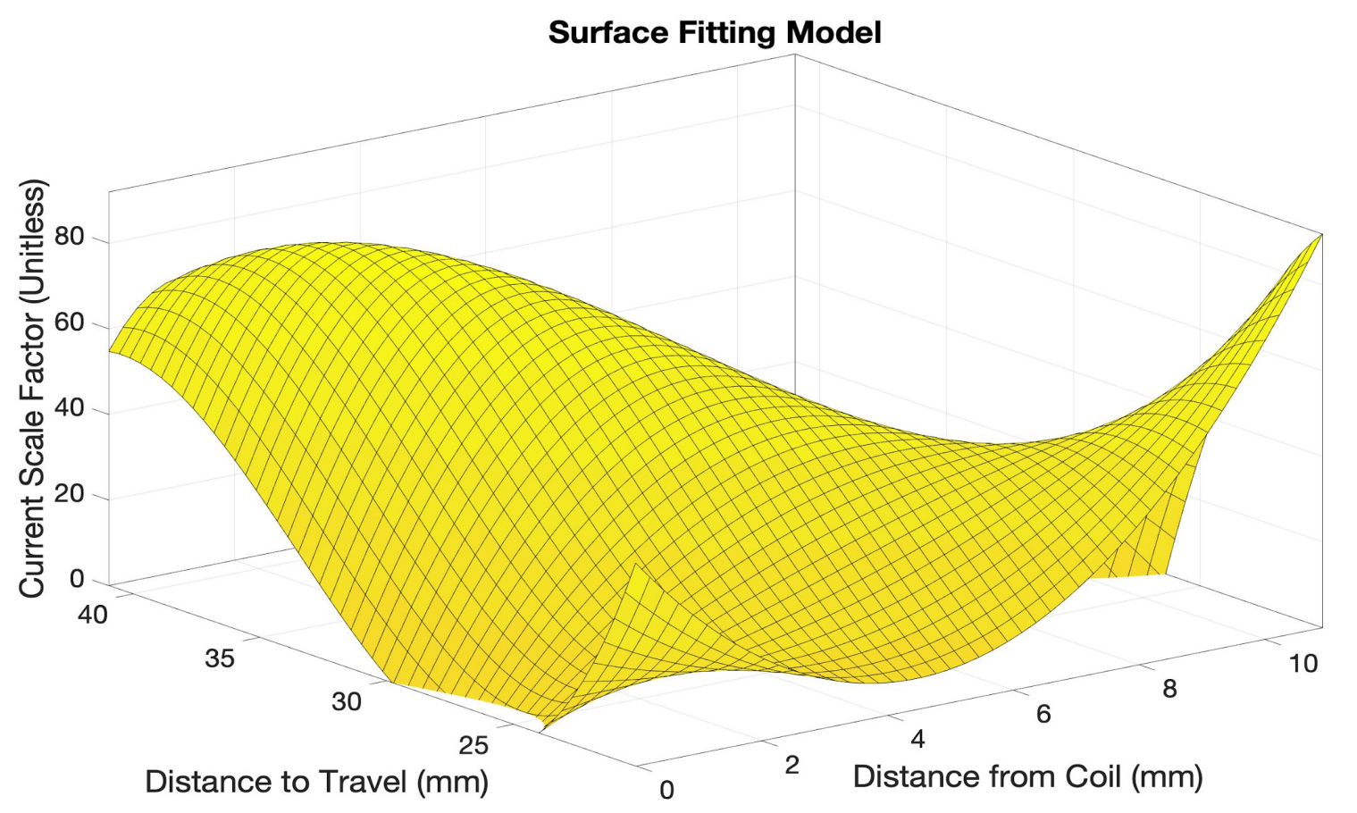

Figure 7. Surface fit particle translation model for a single coil.

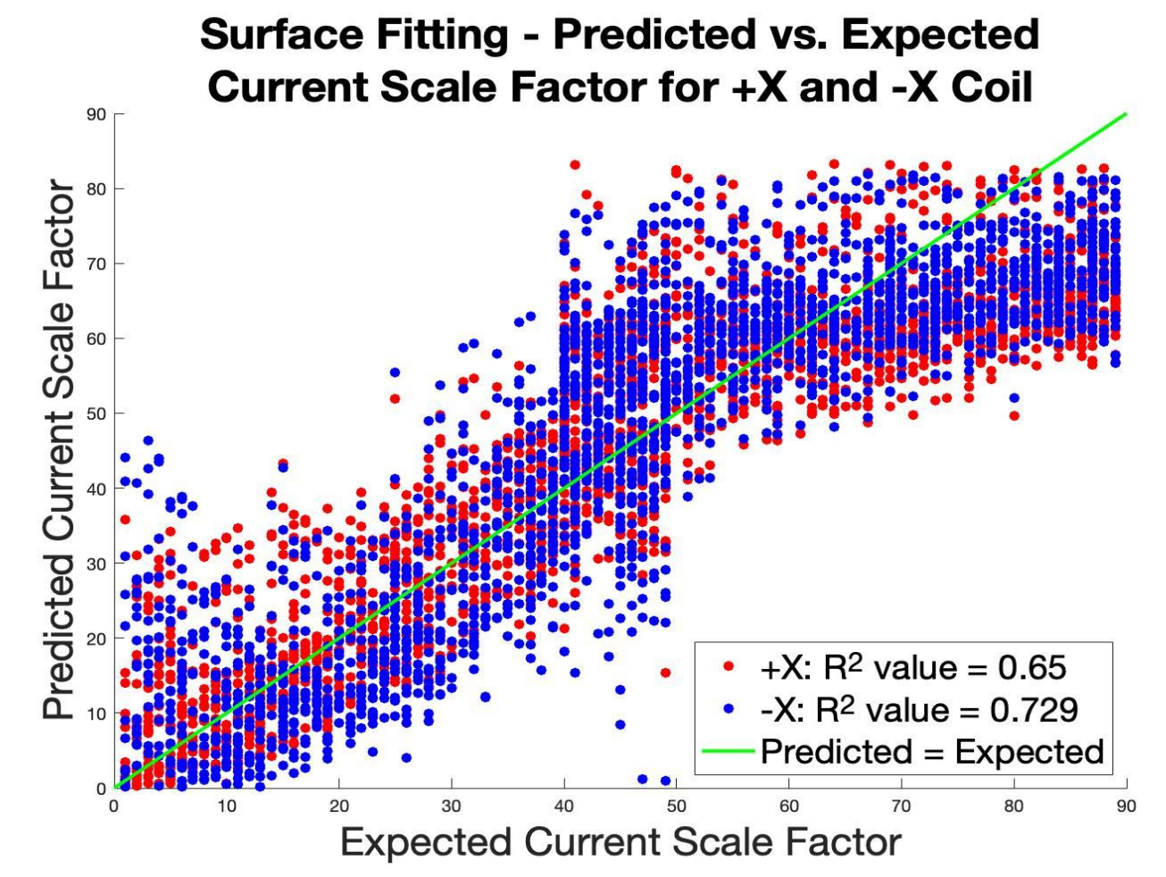

Figure 8. Training regression plot. An ideal regression fit would predict the expected current scale factor with 100% accuracy ($R^2 = 1.0$).

Hardware

1. GUI sends instructions simultaneously to both motor controllers

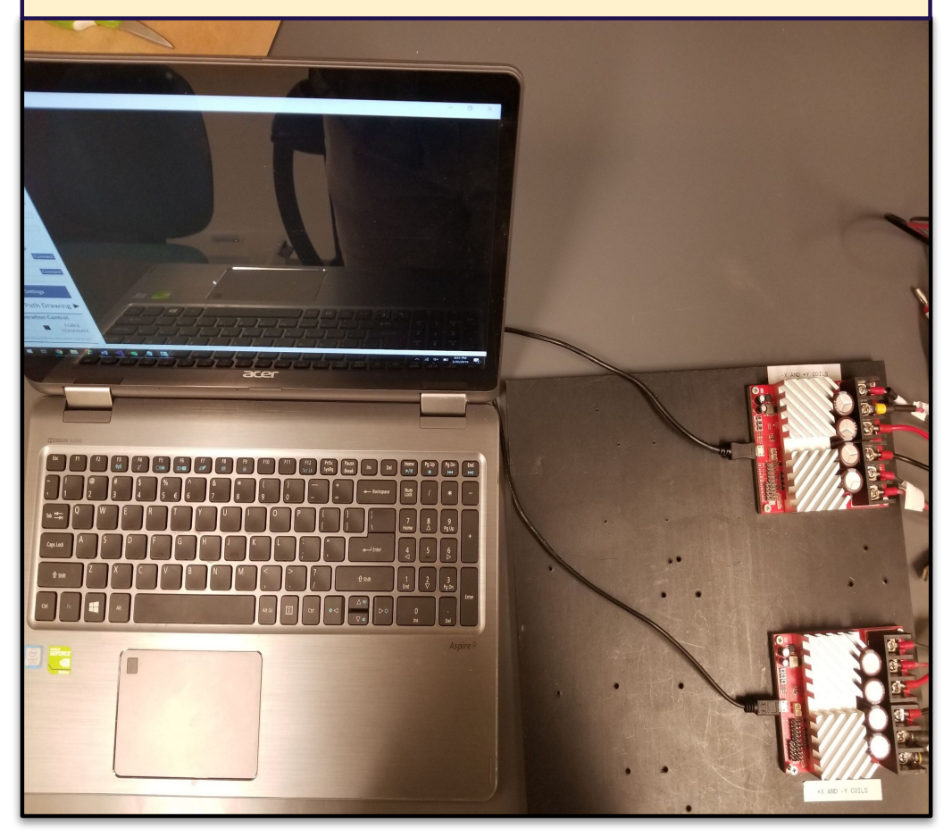

Fig 9. GUI (left) and motor (right) controllers connected via USB

2. Motor controllers run current through connected solenoid coils

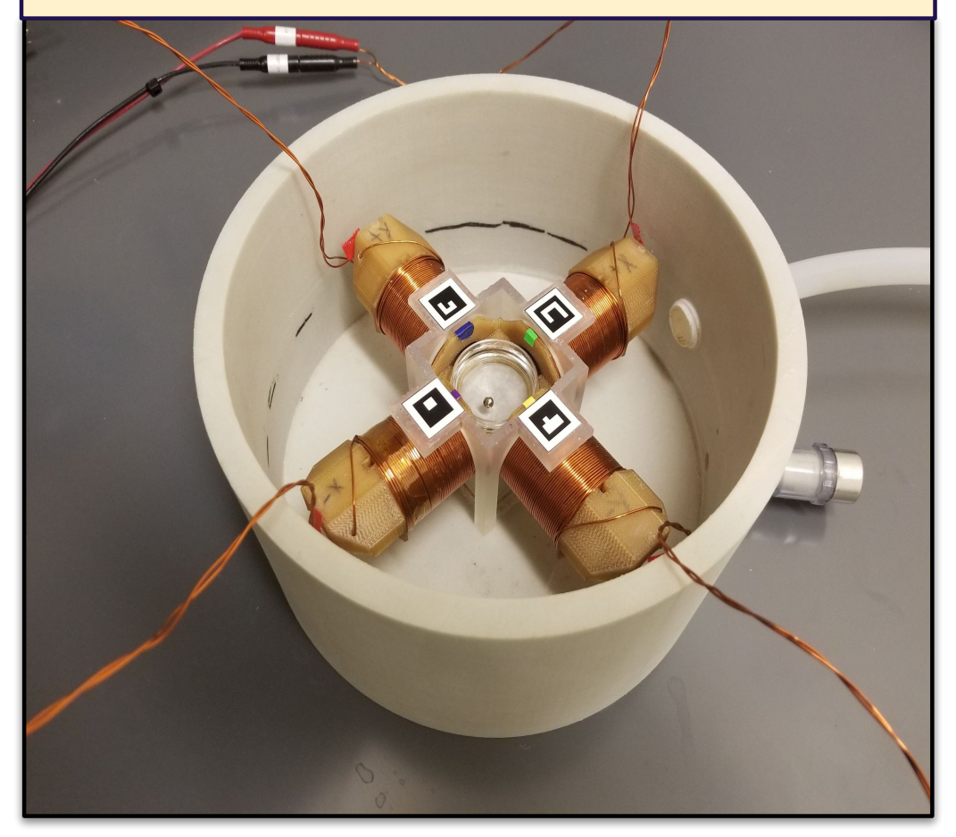

Fig 10. Four coil array with solenoid connections placed within fluid housing

3. Induced magnetic fields translate permanent magnets

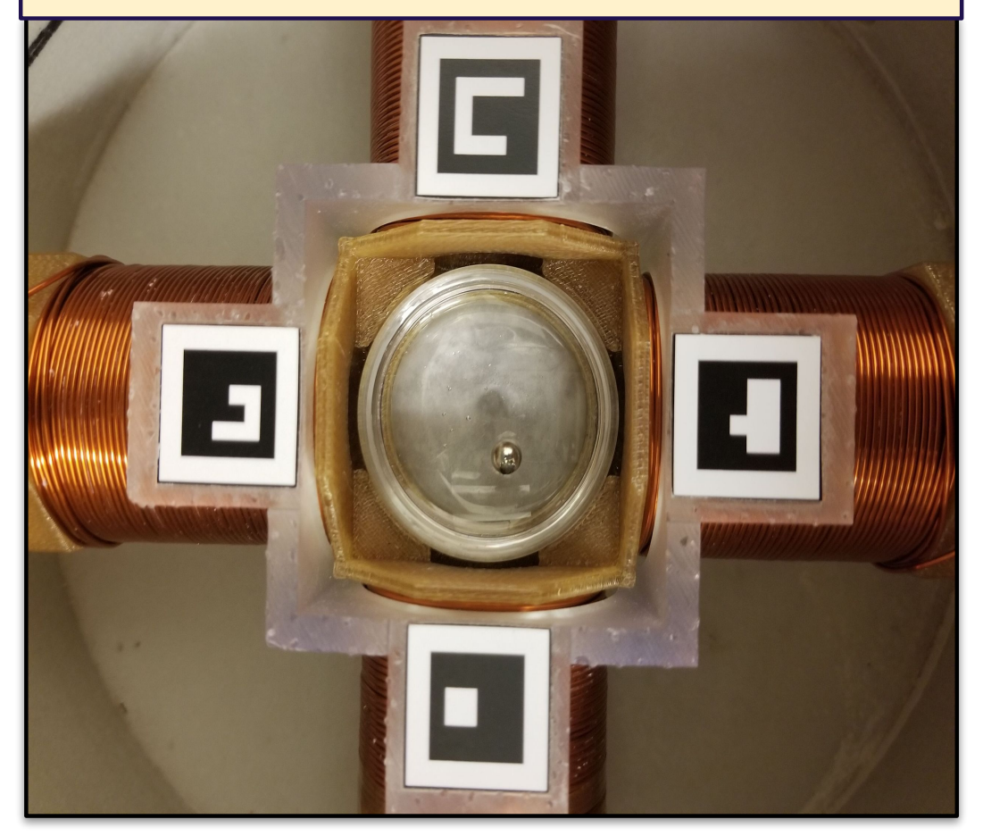

Fig 11. Neodymium sphere magnet suspended in a solution within a petri-dish

Results

Translation Results

- The R^2 values of the surface fitting model were consistently lower than the neural network (Figure 12). Live testing of both translation approaches (given the same desired path with a 1.5 mm tolerance) showed that the neural network allowed for more accurate particle translation along the path than surface fitting.
- To measure the neural network's consistency, 10 particle translation trials were performed using the same desired path (Figure 14). Across the testing period, an average 0.85 mm standard deviation in particle location was observed between trials. The particle's trajectory was found to always be within 1.5 mm of the desired path.

	R^2 Correlation Coefficient	
Trained Coil	Surface Fitting	Neural Network
+X	0.65	0.931
-X	0.729	0.886
+Y	0.735	0.887
-Y	0.827	0.934
AVERAGE	0.73525	0.9095

Figure 12. R^2 of surface fitting model vs neural network model. Higher R^2 implies accurate model predictions.

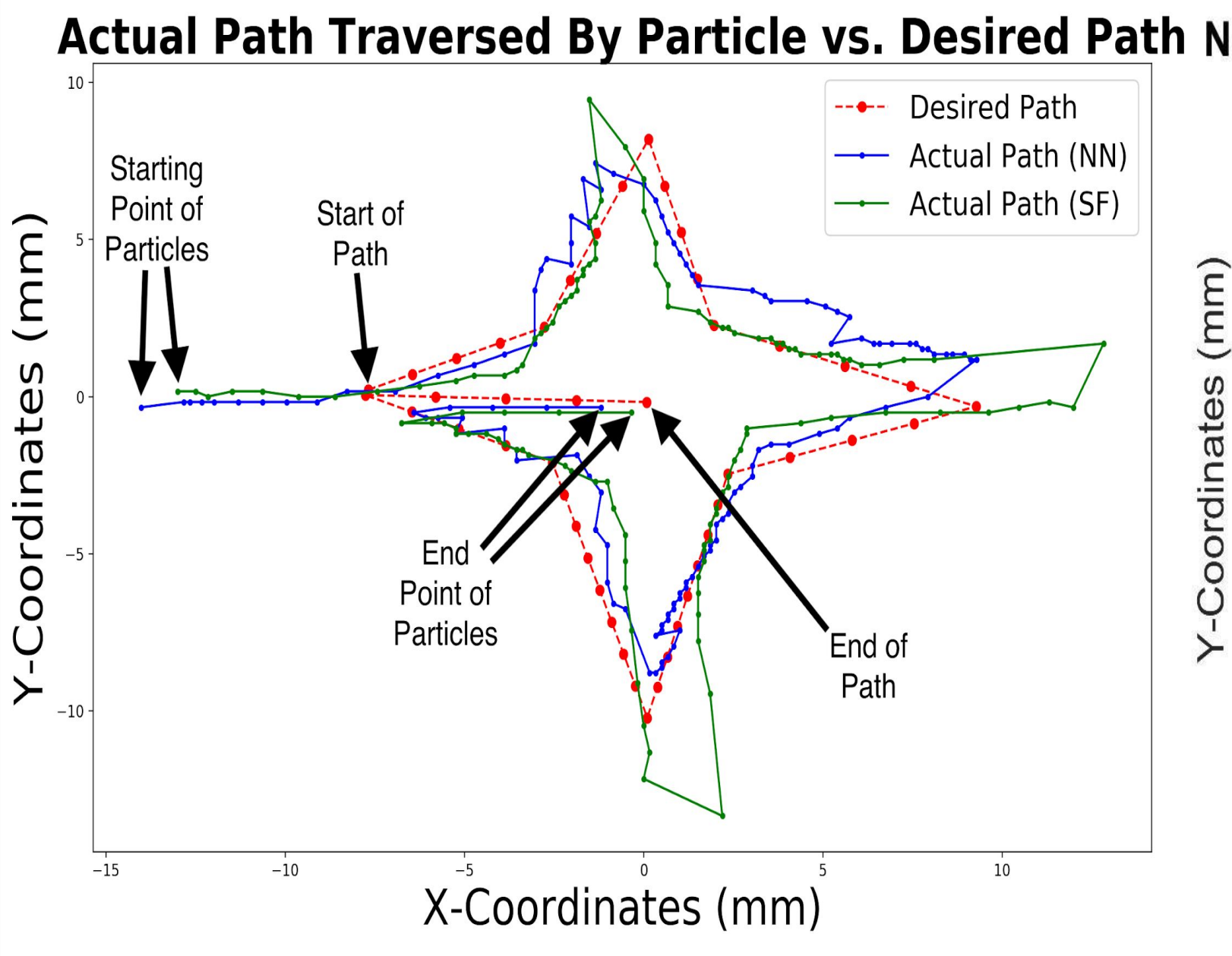

Figure 13. Path traversed by particle using neural network and surface fitting translation vs the desired path of traversal.

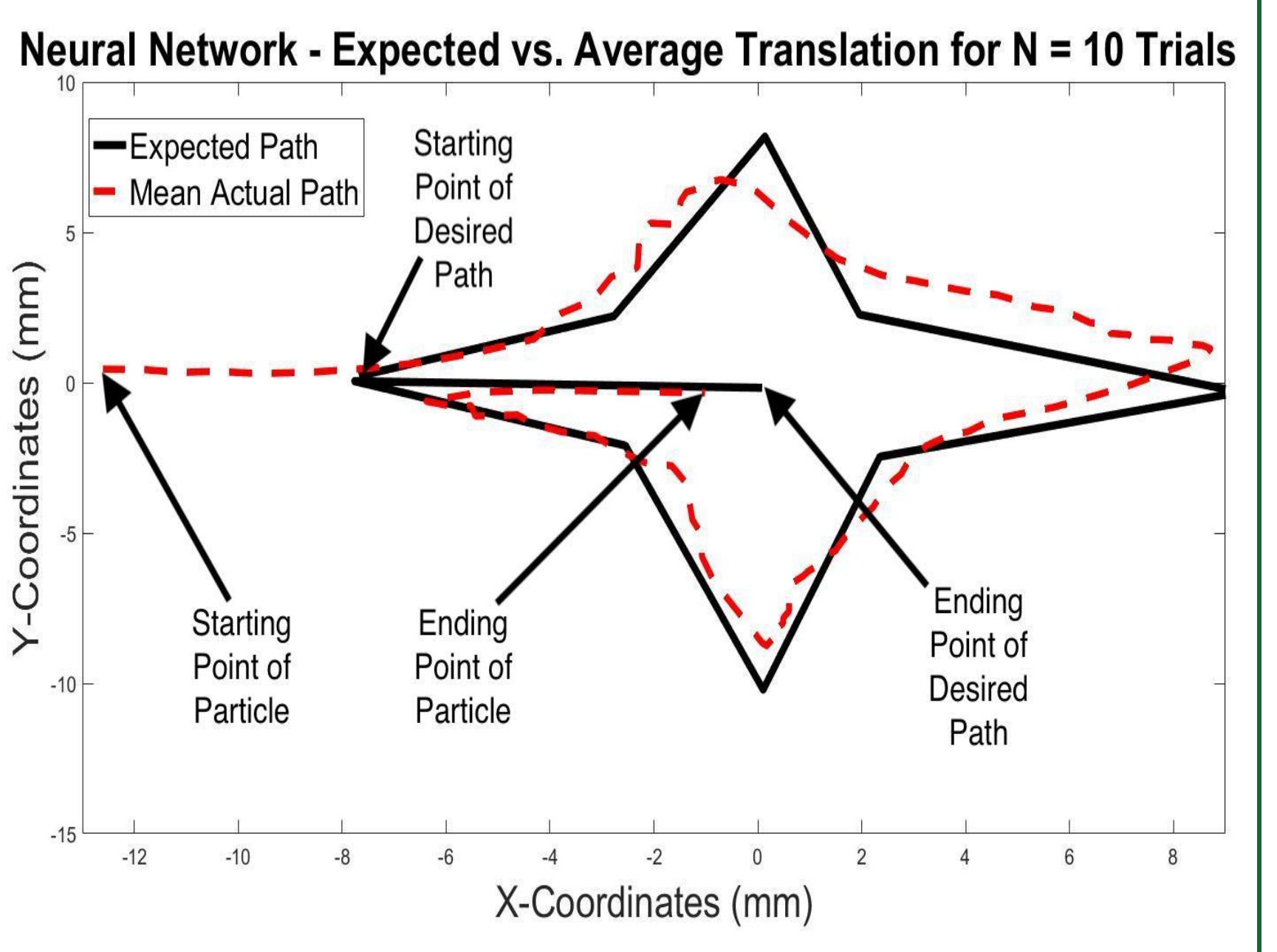

Figure 14. Average neural network model path traversal vs desired for N = 10 trials.

Image Segmentation Results

- Across all lighting conditions, detected particle and coil marker locations deviated less than 0.4 mm across image frames (Figure 15). Ambient lighting was found to be the optimal environment for detection.
- Several segmentation limitations were observed. Coil markers were undetectable if obstructed in any way (i.e. glare). Particle detection was not accurate on the outer edges of the petri-dish and under non-uniform lighting.

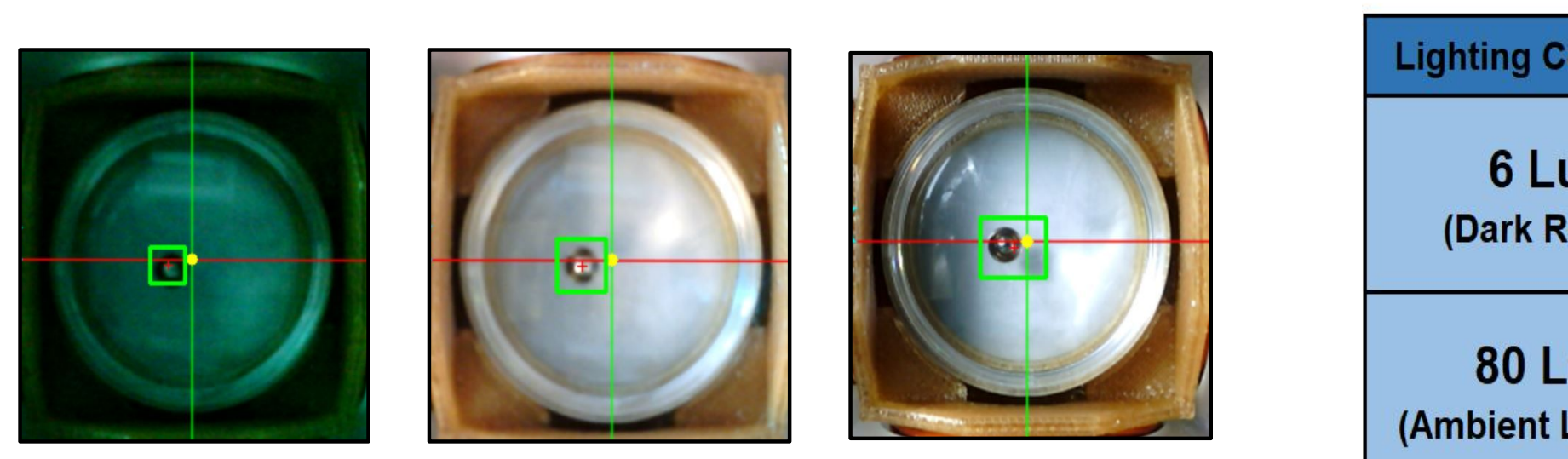

Figure 16. Different lighting conditions. From left to right, the conditions tested are: Dark Room, Ambient Lighting, and under a Direct Light Source.

	Detected Feature Deviation (mm)	
Lighting Condition	Particle Location	Coil Marker Location
6 Lux (Dark Room)	0.3432	0.0049
80 Lux (Ambient Lighting)	0.0521	0
220 Lux (Direct Light Source)	0.1337	0.0266

Figure 15. Detected feature deviation in different lighting conditions for still particle and coil marker locations (mm)

Conclusion and Future Work

MAGNETO was shown to consistently track and accurately guide a magnetic object-of-interest along a user-defined delivery path. System operation can be easily set up and monitored through an intuitive user interface. However, further improvements to translation accuracy can be potentially made through model refinement and altering hardware architecture (e.g. adding in coils to eliminate translation dead zones). Future work consists of porting the system to WMP's future MCS. The next iteration will be capable of processing MR image batches and activating more complex magnet arrays to translate smaller scale particles.

Acknowledgements

We would like to thank:
- **Weinberg Medical Physics** for their funding, provision of hardware, and continual support.
- **Dr. Vasiliki Ikonomidou** and **Mr. Randolph Warren** for their advice regarding image processing and hardware maintenance.
- **Dr. Shani Ross** for facilitating our senior design progress throughout the academic year.
- **GMU Student Support and Advocacy Center** for providing lubricant solution used in particle translation.

References

[1] B. Shapiro, S. Kulkarni, A. Nacev, S. Muro, P. Y. Stepanov, and I. N. Weinberg, "Open Challenges in Magnetic Drug Targeting," Wiley Interdiscip Rev Nanomed Nanobiotechnol, vol. 7, no. 3, pp. 446–457, May 2015.

[2] A. Nacev et al., "Neurostimulation using mechanical motion of magnetic particles wiggled by external oscillating magnetic gradients," in 2017 8th International IEEE/EMBS Conference on Neural Engineering (NER), 2017, pp. 424–427.